

## Tile decoration model of the W-(Al–Co–Ni) approximant

M. MIHALKOVIČ† and M. WIDOM\*‡

†Institute of Physics, Slovak Academy of Sciences, 84511 Bratislava, Slovakia

‡Department of Physics, Carnegie-Mellon University, Pittsburgh,  
Pennsylvania 15213, USA

(Received 15 May 2005; in final form 23 August 2005)

We use *ab-initio* total energy calculations to refine chemical ordering of the W-(Al–Co–Ni) approximant structure and calculate its stability relative to other ternary and binary competing compounds. This approximant structure has 8 Å stacking periodicity along its pseudofivefold axis and can be interpreted as stacking of two identical adjacent 4 Å slabs with stacking vector inclined relative to the pseudofivefold axis. We generalize this stacking motif to model the 8 Å quasicrystal. Starting with 4 Å slabs forming a ‘binary’ (three-level) decagonal tiling, we introduce tile flips between adjacent slabs analogous to the ‘octagon’ tile-reshuffling update move for binary Penrose tiling. These tile flips lower the total energy, implying 8 Å superorder for the quasicrystal at low temperatures, consistent with experiment.

### 1. Introduction

The alloy system Al–Co–Ni [1] is widely studied because it contains thermodynamically stable fivefold and tenfold quasicrystals [2], some of which can be grown as single crystals, suitable for study by electron microscopy [3–5] or X-ray diffraction [6, 7]. The quasicrystal-forming region of the phase diagram turns out to be extremely complicated, containing at least eight distinct variants [8–10]. Of special interest are the ‘basic Ni-rich’ phase, around the composition Al<sub>70</sub>Co<sub>9</sub>Ni<sub>21</sub>, and the ‘basic Co-rich’ phase, around the composition Al<sub>72</sub>Co<sub>17</sub>Ni<sub>11</sub>. These phases are named ‘basic’ because their diffraction patterns contain only basic reflections, while the other modifications contain superlattice peaks.

The ‘basic Ni-rich’ phase has a 4 Å stacking periodicity, while the remaining phases all have 8 Å or higher. Even the 4 Å structure exhibits layers of diffuse scattering suggesting short-range disorder characteristic of an 8 Å modulation. Our discussion of structures utilizes 2 Å slabs consisting of a layer of atoms together with the 1 Å spaces above and below. Depending on reflection symmetries across these at layers, the atoms may be coplanar (forming a flat layer) or slightly displaced off the plane (forming a puckered layer). For example, Al<sub>13</sub>Co<sub>4</sub> is an 8 Å periodic structure which alternates flat and puckered 2 Å layers. Two 2 Å layers form a 4 Å bilayer. For example, the ‘basic Ni-rich’ phase can be described as a periodic

---

\*Corresponding author. Email: widom@andrew.cmu.edu

stacking of identical  $4\text{Å}$  bilayers, while a single period of  $\text{Al}_{13}\text{Co}_4$  consists of two adjacent inequivalent bilayers.

In addition to the quasicrystal phases, some other ternaries exist [11, 12]. Most of these are extensions of binaries into or across the ternary composition space (e.g.  $\beta$  phase with the structure  $\text{Al}(\text{Co},\text{Ni})\cdot\text{cP}2$ ) which we consider as pseudo-binaries. Two intrinsic ternaries exist which have no binary counterparts. These are the X phase [13] with  $4\text{Å}$  periodicity and the W phase [14] with  $8\text{Å}$  periodicity. We are fortunate that they lie close to the quasicrystal phase in composition and that each of their structures has recently been determined.

For complex structures such as quasicrystals, diffraction-data-derived models with mixed or fractional occupancies may hide energetically important occupancy correlations. It becomes essential to discover plausible specific low-energy configurations representative of the ensemble averages accessible to diffraction data experiments. Given such a low-energy structure we wish to derive an ‘idealized’ model that would be transferrable from one approximant to another, yielding reasonable energies for all these structures. In the tile decoration approach, atomic motifs are bound to space-filling tiles according to a decoration rule. From this viewpoint, the refined structure of the W-(Al–Co–Ni) phase provides a unique insight into the detail of the quasicrystalline structure, because it was possible to solve the structure by means of a classical crystallographic approach, because the amount of apparent disorder is tolerably small, and because total energy calculations confirm its plausibility.

Efforts to model the quasicrystals and related approximants rely on planar tilings. Tile vertices can be assigned ‘levels’  $\nu$  in perpendicular space with five allowed values  $(0, \pm 1, \pm 2)$ . Two important types of tiling are hexagon–boat–star (HBS) tilings [15] and binary rhombus tilings [16]. HBS tilings are also known as two-level tilings because they can be formed by starting with a Penrose rhombus tiling, where all vertices occupy just four  $\nu$  levels, and then deleting all rhombus vertices lying on two of the levels. The remaining vertices lie on just two levels (e.g.  $\nu = 0, +1$ ) and form hexagon, boat, and star tiles. Binary rhombus tilings are subsets of four-level tilings in which the vertex  $\nu$  levels are restricted to three values (e.g.  $\nu = -1, 0, +1$ ). Binary tiling are so named because their vertices can be grouped into two sets, type A ( $36$  and  $108^\circ$ , all at  $\nu = 0$ ) and type B ( $54$  and  $72^\circ$  divided among  $\nu = 0, -1$ ).

A plausible model of the ‘basic Ni-rich’ phase has been predicted using first-principles-derived interatomic pair potentials [17] to distribute Al, Co and Ni atoms among sites of an ideal quasilattice [15], leading to decoration rules for HBS tilings of  $4\text{Å}$  bilayers based on an 11-atom decagonal cluster as a fundamental structural unit. Similar methods applied to the Al–Co binary [18] also obtain HBS tilings, but with the pentagonal bipyramid (PB) as a basic structural unit. Recent investigations of Co-rich ternaries provide insight into the link between these two motifs [19] which will be discussed further below.

These clusters play an important role in the following discussion; so we describe them now in detail. The 11-atom decagonal cluster consists of two pentagonal rings of atoms in adjacent  $2\text{Å}$  layers, rotated by  $36^\circ$  with respect to each other. One pentagon contains only Al atoms, while the other layer contains some transition-metal (TM = Co or Ni) atoms. The TM-containing pentagon is centred by a single Al atom. Because it consists of two  $2\text{Å}$  layers, this cluster stacks

with 4 Å periodicity. Likewise, the PB is centred by an Al atom in a flat layer, surrounded by a pentagon of TM atoms. This TM pentagon has a 4 Å edge length and forms the equator of the PB. The puckered layers 2 Å above and below feature PB caps that consist of an Al pentagon centred by a TM atom. Because the height of the PB is 6 Å, it is stacked with 8 Å periodicity by inserting an intervening junction layer containing two or three Al atoms at highly variable positions.

The following section presents our first-principles calculation method. Then, we apply this method to the experimentally reported *W*-phase structure. We find most reported atomic positions are reasonable but a small number are not. Using Monte Carlo simulation we optimize the pattern of Al and TM (i.e. Co or Ni) occupancy in mixed-occupancy sites. We make initial progress on the allocation of TM sites to Co or Ni. Even our most highly optimized structure is high in energy, suggesting that it cannot occur as a stable phase at low temperatures. However, we show the entropy associated with chemical disorder may be sufficient to stabilize the structure at high temperature. Similar conclusions apply to the *X* phase and the  $\beta$  phase.

Our structure model for the *W* phase (figure 1) can be interpreted as tilings of 4 Å bilayer units that are simultaneously two-level HBS tilings and three-level binary tilings. 8 Å periodicity is achieved by introduction of tile flips between adjacent bilayers. Our structure model fills a ‘missing link’ between PB-based models of binary Al-Co, and HBS models of the 4 Å ‘basic Ni-rich’ phase.

## 2. First-principles calculations

We perform first-principles calculations of electronic structure and total energy using the program Vienna *Ab-initio* Simulation Package (VASP) [20, 21], which is based in electronic density functional theory and uses a plane-wave basis for electronic states. We model exchange and correlation potentials via the GGA approximation [22]. Computational efficiency is achieved through the use of projector augmented-wave (PAW) potentials [23], an all-electron generalization of pseudopotentials.

We calculate total energies of every known structure in the the Al-Co-Ni ternary system, including its binary and pure elemental subsystems. Each structure is fully relaxed, in both atomic coordinates and lattice parameters. From the resulting total energies we subtract from the energies of the pure elements in their lowest energy form, to predict the enthalpy of formation,  $\Delta H_{\text{for}}$  at temperature  $T=0$  K. The convex hull of enthalpy versus compositional parameter corresponds to the lowest-enthalpy structures. Convex hull vertices correspond to pure phases, while edges and facets indicate regions of two- or three-phase coexistence. For structures whose energy places them above the convex hull, the corresponding energy difference  $\Delta E > 0$  indicates their degree of instability. If the unfavourable enthalpy is balanced by an entropic term  $TS$ , then their free energy  $G = H - TS$  may be sufficiently low that they become stable at high temperatures  $T > 0$ .

Table 1 presents our data for selected binary and ternary structures. Note that we find no stable ternaries. They all are predicted to decompose into mixtures of various binaries, in apparent contradiction to experimental observation of their formation. We believe that this can be resolved by invoking the entropy of chemical

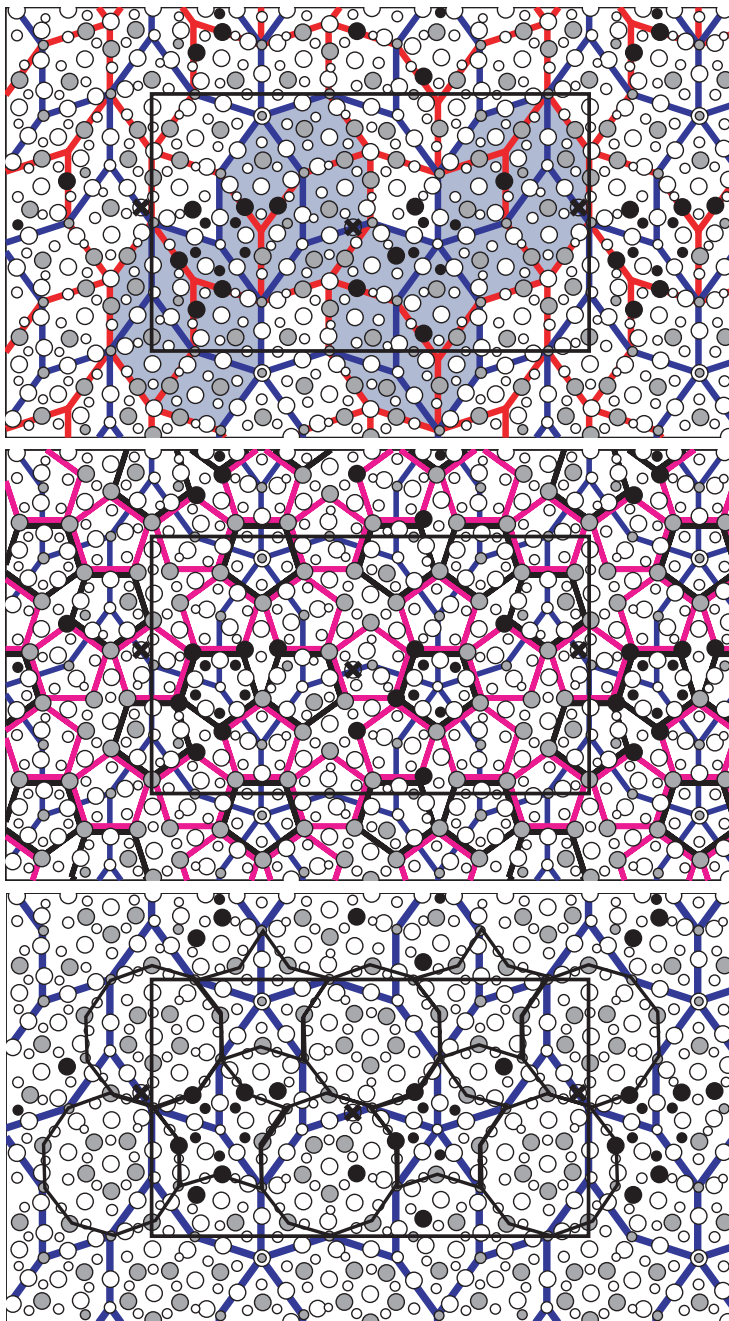


Figure 1. Optimal realization of the W phase. We show only a single 4 Å bilayer. The other is obtained by a translation of  $(a/2, 0, c/2)$ . The upper diagram shows red and blue HBS tilings together outline binary rhombus tiling. Shaded regions are 'octagons' that flip in the adjacent bilayer. The middle diagram shows PB clusters in violet centred on shared vertices of blue and red tilings, Black pentagons are an alternative vertex type of blue tiling. The lower diagram shows 13 Å decagonal clusters of Co-rich decagonal quasicrystal model.

Table 1. Structural Data. TS values are at  $T=1160$  K and include only Co/Ni substitutional entropy.

Compound	Pearson symbol	Atoms per cell (%)			Energies (meV atom <sup>-1</sup> )		
		Al	Co	Ni	$\Delta H_{\text{for}}$	$\Delta E$	$-TS$
Al <sub>9</sub> Co <sub>2</sub>	mP22	18 (82)	4 (18)	0	-350	Stable	0
Al <sub>13</sub> Co <sub>4</sub>	mC102	74 (76)	24 (24)	0	-421	+5.6	0
Al <sub>5</sub> Co <sub>2</sub>	hP28	20 (71)	8 (29)	0	-483	Stable	0
AlCo	cP2	1 (50)	1 (50)	0	-629	Stable	0
Al <sub>3</sub> Ni	oP16	12 (75)	0	1 (25)	-428	Stable	0
AlNi	cP2	1 (50)	0	1 (50)	-677	Stable	0
Al(Co, Ni)	cP2 (cF16)	8 (50)	4 (25)	4 (25)	-632	+20.9	-34.6
W-(Al-Co-Ni)	mC534	190 (72)	55 (21)	20 (8)	-471	+12.7	-19.1
X-Al <sub>9</sub> (Co, Ni) <sub>4</sub>	mC26	18 (69)	3 (12)	5 (19)	-510	+6.1	-10.7

substitution between Co and Ni atoms. We estimate  $S/Nk_B$  as  $2\log 2/2$  for Al(Co, Ni).cP2 (assuming free Co and Ni substitution on half of all sites), as  $0.3 \times (2\log 3/2/3 + \log 3/3)$  for W-(Al-Co-Ni) (assuming free Co and Ni substitution on all TM sites at composition Al<sub>70</sub>Co<sub>20</sub>Ni<sub>10</sub>) and as  $\log 16/26$  for X-Al<sub>9</sub>(Co, Ni)<sub>4</sub> (assuming free substitution of Co and Ni on TM(1) sites) [13]. In each case the substitutional entropy could be sufficient to stabilize the structure at high temperatures, although it is also possible that some of these are merely metastable.

Note that the substitutional entropy cannot stabilize the Al<sub>13</sub>Co<sub>4</sub> phase. Rather, we believe that a combination of an Al vacancy entropy together with vibrational entropy of low-frequency phonons is needed to stabilize this binary compound [24].

### 3. W phase

The experimentally determined W-phase structure is centred monoclinic, with 534 atomic sites per unit cell. Its lattice parameters are  $39.67 \text{ \AA} \times 8.15 \text{ \AA} \times 23.39 \text{ \AA}$ , angle  $\beta = 90.5^\circ$ , identifying it as close to an orthorhombic quasicrystal approximant of type H4B4. It has low symmetry (space group,  $Cm$ , No. 8) and a correspondingly large number of independent orbits. In all there are 131 Al orbits, 11 mixed-occupancy orbits and 57 TM orbits. All sites are claimed to be fully occupied except for one TM orbit which was reported about half-occupied, resulting in a total of about 265 atoms distributed over 267 sites in each primitive cell. The experimentally reported composition is Al<sub>71.8</sub>Co<sub>21.1</sub>Ni<sub>7.1</sub>.

Applying pair potentials [17] to the experimental structure, all sites appear to be energetically plausible except one Al site, which causes a short interatomic distance of about  $2.1 \text{ \AA}$ . We resolved this short distance by relaxing this problematic site using pair potentials.

Fixed-site Monte Carlo simulations [15, 18] swap different chemical species (or vacancies) to select candidate realizations of chemical order on the diffraction-data-refined structure. We examined three variant atomic densities containing 265–267 atoms per primitive cell (the site list contains 267 sites).

We allow slight variation in the composition around the experimentally reported values. In addition we considered variants at 50–50 Co–Ni, plus a couple of binary Al–Co variants. The problematic site mentioned above was a favoured location for a vacancy in structures of less than 267 atoms.

The pair potentials and the diffraction data structure are superbly consistent with each other. All sites identified by experiment as Al remained Al during Monte Carlo annealing, all TM as TM, with the exception of the half-occupied TM site, that Monte Carlo proposes as fully occupied Al (diffraction cannot easily distinguish between these alternatives). Even more surprisingly, the mixed Al–TM sites were resolved by Monte Carlo in exact agreement with the majority species reported by diffraction. When applied to the X phase, the pair potentials reproduce the patterns of Co–Ni order obtained from full *ab-initio* calculations [13]. We are impressed both with the apparent accuracy of the diffraction refinement and with the realism of the pair potentials.

Each optimal structure produced by Monte Carlo simulation was then relaxed with VASP and their energies  $\Delta E$  compared. Our lowest-energy model to date has 265 atoms ( $\rho = 0.071$  atoms  $\text{\AA}^{-3}$ ), at composition  $\text{Al}_{3.0}\text{Co}_{1.0}\text{Ni}_{40}$ . Chemical ordering preserves the reported *Cm* symmetry with the exception of a single Wyckoff site that we refine as mixed Al–Ni (broken mirror). (This also means that all other mixed-occupancy sites resolve to a unique chemical identity at  $T=0$ .) Rms displacements during relaxation are 0.07, 0.04 and 0.07  $\text{\AA}$  for Al, Co and Ni respectively, with a maximum displacement of 0.3  $\text{\AA}$ . Table 1 and figure 1 present the best structure. As mentioned previously, although  $\Delta E > 0$ , it is sufficiently low that disorder in the distribution of Co and Ni on TM sites creates enough entropy that thermodynamic stability is expected at high temperatures.

Two different HBS tilings of edge length 6.5  $\text{\AA}$ , one in blue and the other in red, are inscribed on a 4  $\text{\AA}$  bilayer of our optimal W-phase structure in figure 1. The  $\nu=0$  sites are simultaneously vertices of the blue and red tilings. PB clusters [18, 24] are centred on all these sites, and they are all oriented identically, resulting in (pseudo)fivefold symmetry. The remaining vertices of the blue tiling, at  $\nu = +1$ , frequently are centres of 4  $\text{\AA}$  11-atom decagonal clusters [15]. The remaining vertices of the red tiling are at  $\nu = -2$  and are also frequently centres of 11-atom decagonal clusters.

Evidently, the union of the two tilings (blue+red edges) constitutes a binary rhombus tiling [16], a tiling that was introduced to a model decagonal quasicrystal-forming two-dimensional binary Lennard-Jones alloy. In the W phase, each alternate vertex holds a PB or a non-PB cluster, rather than large and small atomic species as in the original binary tiling. A crucial feature of the binary tiling is the existence of a locally flippable region of three thin and three fat rhombi known as an ‘octagon’ because it is bounded by eight edges. Only octagons whose boundary coincide between octagon one bilayer up and down are considered as ‘flippable’.

When the translation is applied to the first 4  $\text{\AA}$  bilayer of the W phase to produce the second bilayer, completing the 8  $\text{\AA}$  stacking period, we find a fraction of vertices and edges in the second bilayer coincide with positions in the first bilayer. In fact, the net effect of the translation is to introduce tile flips within the shaded octagon regions illustrated in figure 1.

Thus the  $8 \text{ \AA}$  periodicity is achieved by introducing tile flips between adjacent  $4 \text{ \AA}$  bilayers. Our first-principles calculations verify that these tile flips lower the total energy, as is expected since they occur in the experimentally determined structure. Indeed, energy reduction by period-doubling tile flips has been demonstrated in many decagonal structures [25, 26]. In these cases, short-period structures occur as a result of disorder in the period doubling; instead of occurring with strict regularity, tile flips occur at random. One signature of this is that diffuse scattering layers replace the Bragg peaks associated with the longer period. The structure of the  $W$  phase contains many overlapping octagons, not only those that actually flip in the experimentally observed structure, and is indeed a maximal density covering by flippable octagons (four octagons per cell).

The energies and specific structures of other  $W$ -phase realizations are available online [27]. We found that certain Ni-Co and Al-Ni substitutions resulted in fairly low-energy costs, of the order of  $0.1 \text{ eV atom}$  (i.e.  $k_B T$  at typical quasicrystal formation temperatures). Other TM sites, especially those with high Al coordination, have a distinct preference for Co occupancy.

#### 4. Relationship to other phases

TM atoms in the flat layers form a pentagonal network similar to that in orthorhombic and monoclinic  $\text{Al}_{13}\text{Co}_4$ . In  $\text{Al}_{13}\text{Co}_4$ , connecting centres of these clusters form a tiling of hexagons with  $6.5 \text{ \AA}$  edge length. In the  $W$  phase, they form an analogous tiling, containing four Hexagons and five Boats (no stars). Because of the higher TM content of  $W$  phase, there are some TM atoms also inside the pentagons.

There is clearly a significant link between the  $W$ -phase structure and the ‘basic Ni-rich’ phase. For example, 11-atom decagonal clusters, consisting of a central Al atom, an Al pentagonal ring and a mixed Al-TM pentagonal ring are a fundamental building block of the ‘basic Ni-rich’ phase and occur frequently in the  $W$  phase. The approximate topological relationship between the  $W$ -phase structure and the ‘basic Ni-rich’ quasicrystal may be characterized as follows:

- (i) The four-level (decagonal) HBS tiling (‘basic Ni-rich’) phase is replaced by the ‘binary’ three-level HBS ( $W$   $\beta$ -phase).
- (ii)  $4 \text{ \AA}$  PB-like motifs on half of the HBS vertices transforms into proper  $8 \text{ \AA}$  motifs. A channelling mechanism for the transformation (ii) was proposed in [19].

One of the prominent features of the structure are pentagonal columns with  $13 \text{ \AA}$  diameter built from 11-atom decagonal  $\text{Al}_6\text{Co}_5$  cores surrounded by a shell of ten Al, and an outer ring of ten TM. These clusters have essentially  $4 \text{ \AA}$  periodicity, and they also emerged from Monte Carlo simulation attempting to optimize a ‘basic Co-rich’ quasicrystal structure from minimal assumptions using pair potentials [19].

#### 5. Discussion

At present we only have an ensemble-specific  $W$ -phase configurations for which we know the energy of a few variants. To complete our study we need to propose

an idealized model specifying the position and identity of each atom. We would identify the chief structural degrees of freedom and quote an energy cost for each. Hopefully this model could be generalized to describe the Co-rich quasicrystal phase as well. As noted above, the numerous symmetry breakings make it difficult to propose a simple rule. Similarly, the patterns of chemical occupancy are closely tied to the details of the local tiling, with Ni atoms able to substitute either for Co or for Al in certain circumstances.

Although our understanding of W-(Al-Co-Ni) remains incomplete, we find that it provides a link between Al-Co binary structures of 8 Å periodicity and the ‘basic Ni-rich’ quasicrystal phase of 4 Å periodicity. Specifically, the 8 Å periodicity allows binary-tiling flips between adjacent bilayers. When these flips occur regularly, 8 Å periodicity results and both PB and 11-atom decagonal clusters are observed. When they occur randomly, the PB clusters are broken, while the 11-atom decagons are preserved, and 4 Å periodicity results.

### Acknowledgements

This work was supported in part by National Science Foundation grant DMR-0111198. We acknowledge useful discussions with C.L. Henley. M. M. also acknowledges support from grants VEGA-2/5096/25, APVT-51021102, APVT-51052702 and SO-51/03R80603. Some of the *ab-initio* calculations were carried out under EC-funded project HPC-Europa, contract 506079.

### References

- [1] T. Gödecke and M. Ellner, *Z. Metallkd.* **87** 854 (1996).
- [2] A.-P. Tsai, A. Inoue and T. Masumoto, *Mater Trans. Japan Inst. Metals* **30** 463 (1989).
- [3] K. Hiraga, F.J. Lincoln and W. Sun, *Mater Trans. Japan Inst. Metals* **32** 308 (1991).
- [4] E. Abe, K. Saitoh, H. Takakura, *et al.*, *Phys. Rev. Lett.* **84** 4609 (2000).
- [5] Y. Yan, S.J. Pennycook and A.-P. Tsai, *Phys. Rev. Lett.* **81** 5145 (1998).
- [6] H. Takakura, A. Yamamoto and A.-P. Tsai, *Acta Crystallogr. A* **57** 576 (2001).
- [7] A. Cervellino, T. Haibach and W. Steurer, *Acta Crystallogr. B* **58** 8 (2002).
- [8] S. Ritsch, C. Beeli, H.-U. Nissen, *et al.*, *Phil. Mag. Lett.* **78** 67 (1998).
- [9] D. Joseph, S. Ritsch and C. Beeli, *Phys. Rev. B* **55** 8175 (1997).
- [10] R. Luck, M. Scheffer, T. Gödecke, *Matter. Res. Soc. Symp. Proc.* **553** 25 (1999).
- [11] T. Gödecke, M. Scheffer, R. Luck, *et al.*, *Z. Metallkd.* **89** 687 (1998).
- [12] M. Scheffer, T. Gödecke, R. Luck, *et al.*, *Z. Metallkd.* **89** 271 (1998).
- [13] S. Katrych, M. Mihalkovič, V. Gramlich, *et al.*, *Phil. Mag.* **86** 451 (2006).
- [14] K. Sugiyama, S. Nishimura and K. Hiraga, *J. Alloys and Compounds* **342** 65 (2002).
- [15] M. Mihalkovič, I. Al-Lehyani, C. Cockayne, *et al.*, *Phys. Rev. B* **65** 104 205 (2002).
- [16] M. Widom, D.P. Deng and C.L. Henley, *Phys. Rev. Lett.* **63** 310 (1989).
- [17] I. Al-Lehyani, M. Widom, Y. Wang, *et al.*, *Phys. Rev. B* **64** 075 109 (2001).
- [18] E. Cockayne and M. Widom, *Phil. Mag. A* **77** 593 (1998).
- [19] N. Gu, C.L. Henley and M. Mihalkovič, *Phil. Mag.* **86** 593 (2006).
- [20] G. Kresse and J. Hafner, *Phys. Rev. B* **47** RC558 (1993).
- [21] G. Kresse and J. Furthmüller, *Phys. Rev. B* **54** 11 169 (1996).
- [22] J. Perdew and Y. Wang, *Phys. Rev. B* **45** 13 244 (1992).



- [23] G. Kresse and J. Joubert, Phys. Rev. B **59** 1758 (1999).
- [24] M. Mihalkovič and M. Widom, to be published (2005).
- [25] C.L. Henley, M. Mihalkovič and M. Widom, J. Alloys and Compounds **342** 221 (2002).
- [26] M. Mihalkovič and M. Widom, Phys. Rev. Lett. **93** 095 507 (2004).
- [27] M. Mihalkovic and M. Widom, alloy database. Available online at: <http://alloy.phys.cmu.edu> (accessed 2005).